Journal of
Water & Climate Change

IWA PUBLISHING

Journal of Water and Climate Change Vol 15 No 3, 1054 doi: 10.2166/wcc.2024.468

Spatiotemporal variation of projected drought characteristics in Iran under climate change scenarios using CMIP5-CORDEX product

Alireza Ghaemi[a], Seyed Arman Hashemi Monfared[a,b,*], Abdolhamid Bahrpeyma[a], Peyman Mahmoudi[c] and Mohammad Zounemat-Kermani[d]

[a] Department of Civil Engineering, University of Sistan and Baluchestan, Zahedan, Iran
[b] School of Engineering, Cardiff University, Cardiff, UK
[c] Department of Physical Geography, University of Sistan and Baluchestan, Zahedan, Iran
[d] Department of Water Engineering, Shahid Bahonar University of Kerman, Kerman, Iran
*Corresponding author. E-mail: hashemi@eng.usb.ac.ir, hashemimonfaredsa@cardiff.ac.uk

SAH, 0000-0001-5300-9808

ABSTRACT

This study aims to assess the change of drought characteristics (intensity, duration, and frequency) under the effect of climate change in Iran using the modified standardized precipitation index (MSPI) and theory of runs on annual and seasonal scales for three near-future, mid-future (MF), and far-future climates. Hence, regional climate models extracted from South Asia-Coordinated Regional Climate Downscaling Experiments (CORDEX-SA) are applied. Regarding the result, MSPI could assign the standardized precipitation index (SPI) values better than the conventional form of SPI during the historical period (HP). The outcomes revealed that the northeast stations will experience a decrease in intensity (up to 24.57% in MF compared with HP) until 2100 at seasonal timescale, while the duration and frequency of drought will be increased. Although the greatest increase in intensity changes of droughts (up to 91%) until the end of the century will happen in the eastern and southwestern regions of Iran, these regions will face the maximum decrease in the duration (−30.54%) and frequency (−25%) of droughts compared with HP at seasonal timescale. In addition, regarding the outcomes of this study, strategies can be adopted to better manage water resources for various regions of Iran.

Key words: climate change, CORDEX-South Asia, drought, modified standardized precipitation index (MSPI)

HIGHLIGHTS

- The standardized precipitation index (SPI) is modified based on the suitable probability distribution function, existence of zero precipitation values, and arrangement of precipitation time-series.
- The drought characteristics are computed using theory of runs and modified SPI.
- Changes in Iran's drought characteristics (until 2100) are determined for annual and seasonal timescales.

GRAPHICAL ABSTRACT

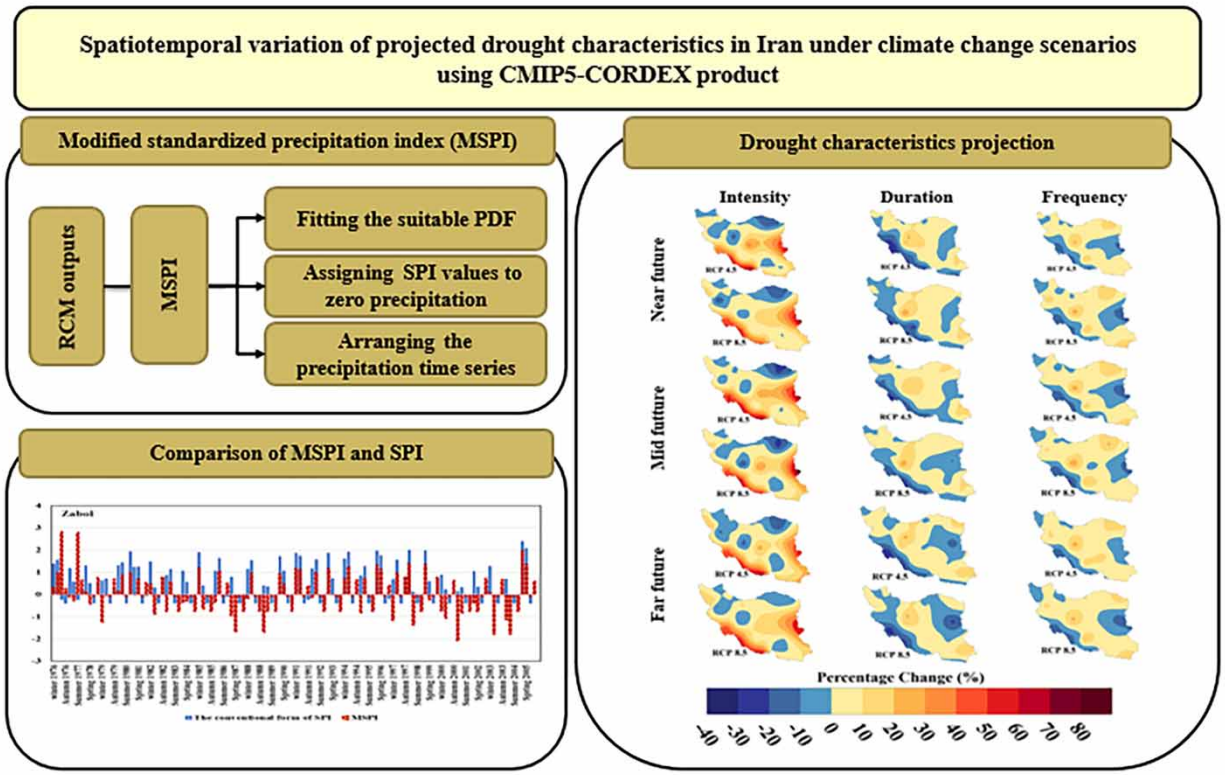

1. INTRODUCTION

Nowadays, climate change caused by global warming is the most serious environmental challenge that the world is facing. Temperature increment owing to global warming causes an increase in evapotranspiration and atmospheric water-holding capacity. The result of this increase can be a change in the magnitude, duration, and frequency of precipitation and a change in their spatial–temporal distribution. Therefore, the expectation of the occurrence of more severe and frequent hydrological hazards, such as droughts and floods, can be one of the primary effects of this global climate change (Dai 2011, 2012; IPCC 2012; Trenberth *et al.* 2014; Mahmoudi & Rigi Chahi 2019).

Aridity as one of the permanent characteristics of climate is known regarding the long-term climatic conditions over a special region, whereas a temporary deviation from normal weather conditions is called drought and can occur in various climates. It is anticipated that drought and aridity increase owing to climate change. Consequently, it may have remarkable subsequences for ecosystems (Karamouz *et al.* 2013; Araghi *et al.* 2018). A wide range of studies have investigated the trend of changes in drought characteristics including the intensity, duration, as well as frequency of droughts on global, regional, and local scales, and can be classified into two general categories. The first category is studies that have examined the changes in three drought characteristics based on historical records, and the second category is studies that have simulated the same changes for the future. Studies that have studied the changes in the intensity, duration, and frequency of droughts based on historical records on a global scale have reported that no specific pattern of behavior has yet been observed on a global scale. On regional scales, temporal and spatial changes of droughts have been established in numerous studies. Some of these studies claim that the frequency and intensity of droughts have increased since the end of the 20th century and others claim that the frequency and intensity of droughts have decreased in some parts of the world (Gu *et al.* 2015; Romanowicz *et al.* 2016; Shahid *et al.* 2016; Swain *et al.* 2016; Wang *et al.* 2016; Fang *et al.* 2018).

In Iran, a large number of studies (e.g. Bari Abarghouei *et al.* 2011; Nouri & Homaee 2020) have focused on changes in drought characteristics. For instance, Nouri & Homaee (2020) studied the trend of drought intensity in Iran using the two indices of standardized precipitation index (SPI) and standardized precipitation–evapotranspiration index (SPEI) on four

timescales of three, six, 12, and 24 months. The results of the study disclosed that, based on the SPI, 76%, and based on the SPEI, 85% of the studied stations had a decreasing trend.

Previous studies (e.g. Tabari & Willems 2018; Yao *et al.* 2020; Zhai *et al.* 2020; Su *et al.* 2021; Waseem *et al.* 2021) that have simulated changes in drought characteristics (intensity, duration, and frequency of droughts) for the future climate under the influence of global warming show that despite significant regional changes, a global drying trend is predicted during the 21st century. The studies that have investigated drought indices under the conditions of climate change, for future periods, on the territorial scale of Iran, are very limited. Khazanedari *et al.* (2009) used the LARS-WG statistical model to project the drought situation in Iran in the next 30 years and disclosed that most parts of the country will face severe or very severe drought by 2039. Zarrin & Dadashi-Roudbari (2021a), by projecting consecutive wet and dry spells in Iran, concluded that the anomaly of consecutive dry spells is increasing as a standard index for short-term droughts under climate change conditions in Iran. Zarrin & Dadashi-Roudbari (2021c) also stated that dry days will increase by 7.5% and the length of dry spells by 28.8% until the year 2100. Senatore *et al.* (2019) also projected a 20% decrease in Iran's precipitation for the period of 2070–2099 under the RCP4.5 scenario based on the climate data of the South Asia-Coordinated Regional Climate Downscaling Experiments (CORDEX-SA) project. This 20% decrease in Iran's precipitation will eventually lead to more severe droughts for Iran, based on the self-calibrating Palmer drought severity index.

Iran is one of the arid and semi-arid countries with precipitation of roughly 250 mm (about one-third of the global precipitation), and dryness is one of the significant features of its climate. About 175 mm of it returns to the atmosphere through evaporation and transpiration, and only about 14 mm of precipitation penetrates the ground, which is the main source of supplying a large part of Iran's water, which is underground reserves. Any change in the different characteristics of droughts in Iran under climate change in the future can highlight complicated challenges of water supply for competitive uses in different parts of Iran at a time of severe water shortage. This complexity will increase when there are numerous concerns about the uselessness of current drought management practices in Iran, which are mainly based on crisis management.

On the other hand, despite the various advantages of SPI in drought monitoring, this index has some limitations (including considering the appropriate probability distribution (PD), existence of zero values in precipitation time-series, and suitable arrangement of precipitation time-series), which lead to incorrect calculation of SPI values. Hence, this study attempts to assign SPI values based on the existence of zero precipitation, the most appropriate probability distribution function (PDF) as well as a proper arrangement for precipitation time-series as the first aim of this study. After that, based on the background of the research presented, the purpose of this article is to study the effect of climate change on the temporal–spatial characteristics of the intensity, duration, and frequency of droughts in Iran on two seasonal and annual timescales, which has been less discussed in previous studies.

2. MATERIALS AND METHODS

2.1. Study area

Iran as a vast country with an area of 1,648,195 km^2 spread between latitudes 25 to 40° north and longitudes 44 to 63° east in the desert belt of the northern hemisphere in southwest Asia (Figure 1(a)). Moreover, there are six main hydrological catchments in Iran as shown in Figure 1(b). Owing to the specific geographical and topographical features of different regions of Iran, various climates prevail over it. Regarding the Köppen–Geiger climate classification (Kottek *et al.* 2006), Iran is divided into 11 climate categories as shown in Figure 1(c). The spatial distribution (SD) of precipitation is remarkably varied in different areas of this country with the maximum and minimum average annual precipitation on Caspian Sea shores (1,800 mm) and arid regions (less than 50 mm), respectively (Figure 1(d)).

2.2. Data

The data required for this research include two groups of observational data and simulated data, which will be introduced further. The first group was related to the monthly precipitation data of 39 synoptic stations for 30 years (1976–2005), which was provided by the Iran Meteorological Organization. The statistical indices of annual precipitation for the considered stations during the historical period (HP) are presented in Table 1.

The SD of the long-term average of seasonal precipitation in Iran during the HP is represented in Figure A1 of the Supplementary Material. Regarding Figure A1, the SD of the long-term average of seasonal precipitation was different in various regions in such a way that expect Caspian Sea catchments (northern regions of Iran), long-term average precipitation

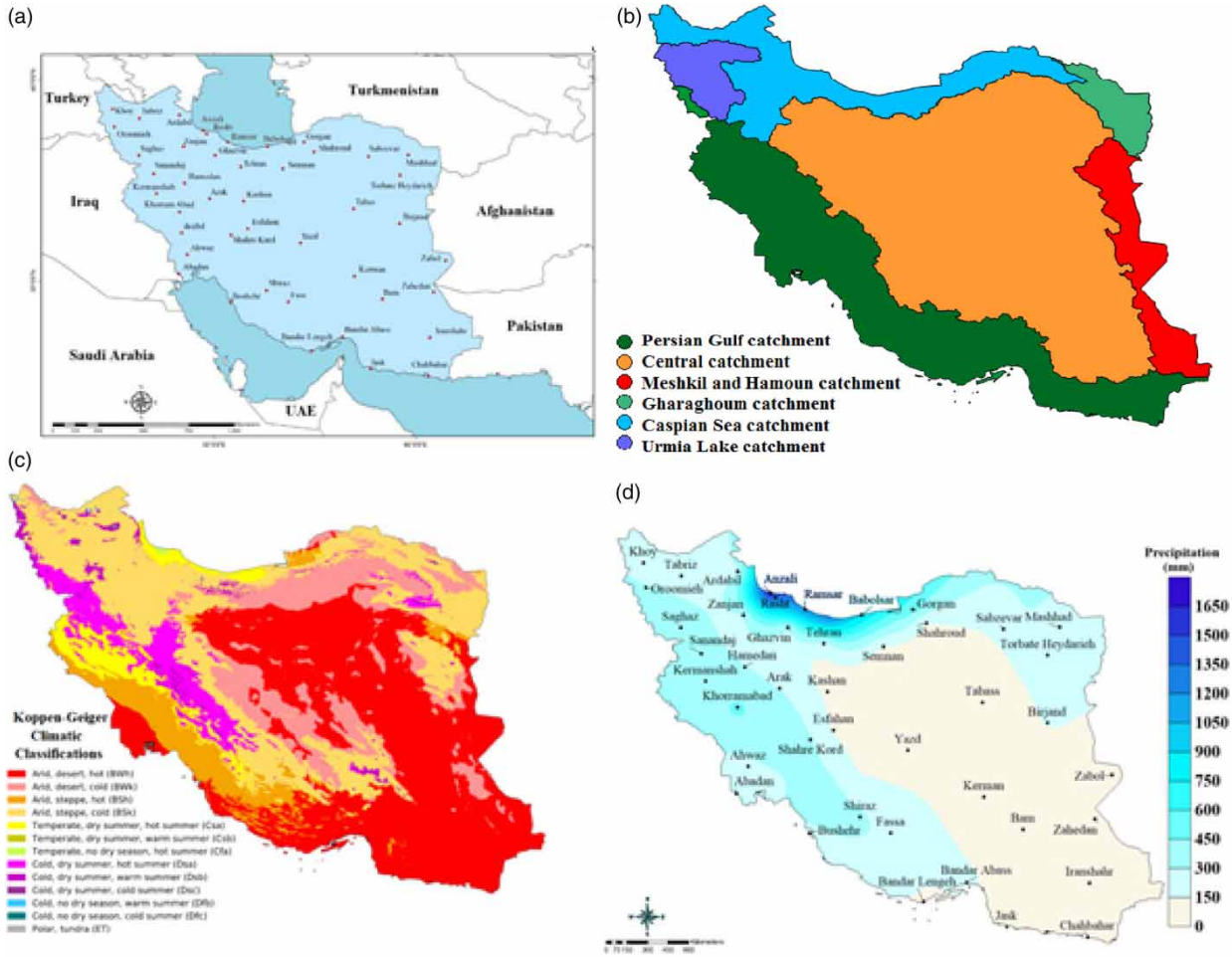

Figure 1 | (a) Geographical location map of Iran in southwest Asia, (b) main hydrological catchments in Iran, (c) climatic classification map of Iran based on the Köppen–Geiger method, and (d) spatial distribution map of Iran's average annual precipitation.

for each season was less than 100 mm. In addition, winter and summer were the rainiest and driest seasons in Iran, respectively.

The coefficient of variation (CV) of precipitations at seasonal and annual timescales during the HP is indicated in Figure A2 of the Supplementary Material. The CV as an indicator is indicative of the changes in the annual precipitation rates in contrast to their long-term average as a percentage. From Figure A2, it is obvious that winter and summer as the rainiest and driest seasons gained the lowest and highest CV values, respectively. Moreover, the maximum CV values for summer and autumn were obtained by the Persian Gulf (e.g. Bushehr and Ahwaz) and Meshkil and Hamoun (e.g. Chabahar) catchments of Iran. The minimum CV was gained by the northern regions such as Rasht station. The stations with higher CV values than others are those with greater changes in their annual precipitation rates in contrast to the long-term average from year to year. This indicates the uncertainty of precipitation as one of the primary sources of water resource supply in these stations (such as in the southeast regions of Iran). The stations with lower CV represent various conditions compared with the other stations. In these stations, the changes in the annual precipitation are too low from year to year and the certainty of precipitation as a primary source of water resource supply is very high (such as for the stations located in the south of the Caspian Sea's shorelines).

Whenever the left and right of a distribution are not mirror images, the distribution can be asymmetrical. The skewness values at seasonal and annual timescales during the HP are revealed in Figure A3 of the Supplementary Material. According to Figure A3, the magnitude of skewness provided for the studied stations indicated that nearly 10% of the stations had negative skewness while the remaining stations had positive. The skewness represents the deviation of

Table 1 | Statistical indices of annual precipitation (mm) for the considered stations during HP

No	Name	Average	Standard deviation	Maximum	Minimum
1	Bandar Anzali	1,783.39	312.76	2,619.9	1,073
2	Ardebil	306.26	78.23	526.5	165.6
3	Babolsar	943.48	150.63	1,306.6	683.1
4	Ramsar	1,217.52	289.01	1,774.8	828.9
5	Abadan	170.78	54.95	292.5	87
6	Ahwaz	243.90	68.46	420.4	84.6
7	Arak	324.72	89.23	497.5	178.3
8	Bam	59.27	26.37	126.8	19.8
9	Bandar Abbas	205.82	118.91	464.8	31.8
10	Bandar Lengeh	153.77	99.51	374.2	7.9
11	Birjand	173.16	52.80	259	52.6
12	Bushehr	276.38	123.94	596.1	109.4
13	Esfahan	126.75	46.96	213.1	58.6
14	Fasa	318.41	122.26	581.8	132.4
15	Qazvin	329.54	79.93	475.3	175.7
16	Gorgan	565.34	88.13	756.9	397
17	Iranshahr	110.99	62.90	258.8	9.1
18	Kashan	137.87	49.74	232.6	76
19	Kerman	142.50	35.33	211.2	74.1
20	Kermanshah	434.06	102.83	727.5	238.1
21	Khoram abad	501.07	135.48	880	288.3
22	Khoy	284.22	80.40	530.6	171.6
23	Mashhad	271.82	79.12	431.8	134.6
24	Urmia	322.30	104.92	608.4	169.8
25	Rasht	1,374.02	262.61	1,947.3	892.4
26	Sabzevar	205.59	56.37	296.7	94.8
27	Saghez	499.31	134.83	818.2	258.7
28	Sanandaj	463.60	127.75	733.3	211.2
29	Semnan	145.45	40.89	260.5	55.9
30	Shahre Kord	336.12	92.69	541.2	178.4
31	Shahroud	162.28	49.81	288.7	74.4
32	Shiraz	348.82	104.30	599.2	162.4
33	Tabriz	265.80	68.31	403.6	129.4
34	Tehran	245.85	64.06	365.2	108
35	Yazd	64.69	26.32	113.7	29.7
36	Zabol	62.67	37.17	166.7	8.1
37	Zahedan	75.44	46.87	217.1	13.3
38	Zanjan	295.37	61.65	410.8	169.7
39	Chabahar	115.47	94.41	399.9	1.4

the dataset toward one margin of the symmetrical distribution. Skewness values between −0.1 and 0.1 indicate that the data curves are symmetrical. Accordingly, the Kerman and Sanandaj stations with skewness = 0.08 were selected as two symmetrical annual precipitation data curves. A smaller skewness value than −0.5 or larger value than 0.5 for annual

precipitation average revealed that the dataset has a significant skewness. Among the considered stations, only Birjand station had a large negative skewness (−0.73), whereas 15 stations were found with large positive skewness during the HP. It can be deduced that the skewness values of the annual precipitation average rates were positive. Therefore, these stations had significant potential for a greater tendency toward drought occurrence. As shown in Figure A3, the most of stations in Iran had positive skewness on a seasonal timescale. Furthermore, it is proposed that stations had highest skewness values in summer due to the dry nature of this season.

A study of zero precipitation at both annual and seasonal timescales also indicated that the maximum number of zero precipitations happened during summer owing to its dry nature. Moreover, the eastern and southwest regions of Iran such as Zabol and Bushehr had the remarkable zero precipitation in summer during HP. In addition, it can be said that all stations in Iran experienced precipitation during winter and spring (Figure A4, Supplementary Material).

The second group is the simulated precipitation data of the RegCM 4.4 regional climate model (RCM) related to the CORDEX-SA on a monthly scale. The driving fields used in this dynamical downscaling are from six general circulation models (GCMs), all of which belong to the Coupled Model Intercomparison Project Phase 5 (CMIP5) and are as follows: CCCma-CanESM2, Centre National de Recherches Meteorologiques (CNRM)-Centre Europeen de Recherche et Formation Avancees en Calcul Scientifique (CERFACS)-CNRM-CM5, Commonwealth Scientific and Industrial Research Organisation (CSIRO)-Queensland Climate Change Centre of Excellence (QCCCE)-CSIRO-Mk3-6-0, NOAA-GFDL-GFDL-ESM2M, IPSL-IPSL-CM5A-MR, and MP I-M-MPI-ESM-LR. All these data are available from the website of the Climate Change Research Center of the Indian Institute of Tropical Meteorology at http://cccr.tropmet.res.in/home/index.jsp.

The simulated data cover the HP (1976–2005) and three future climate periods, which are named near-future (NF) climate (2010–2039), mid-future (MF) climate (2040–2069), and far-future (FF) climate (2070–2099) under two representative concentration pathway scenarios, namely, RCP4.5 (corresponding to about 2 °C global warming by the end of this century) and RCP8.5 (continuation of business as usual until the end of this century). The spatial resolution of these data is also about 0.44°. Table 2 indicates the general characteristics of all GCMs, RCMs, and their spatial resolution.

2.3. Selecting the suitable probability distribution function

The long-term precipitation values for each station must be fitted with the PD applicable to that time series at various timescales to correct the output of the RCMs and calculate the SPI. In SPI computation, the gamma PD has been recommended by numerous researchers as needed for this match, including McKee *et al.* (1993, 1995). However, precipitation values in arid and semi-arid areas are not evenly distributed and have a considerable skewness, especially at shorter timescales. The skewness is a significant obstacle to computing the SPI for certain climatic regions using the gamma distribution. Hence, various PDFs were chosen and fitted to the precipitation values to assess their applicability in SPI adjustment for these climatic zones.

The Kolmogorov–Smirnov test has been employed to assess how well various PDs fit into the distribution of observational data. For this test, the data are divided into various groups. Equation (1) represents the test's statistics, which demonstrate the

Table 2 | CORDEX-SA simulations: RCMs, forcing GCMs, and their resolution

RCM institution(s)	RCM	GCM	GCM institution(s)	Resolution
Indian Institute of Tropical Meteorology (IITM)	RegCM 4.4	CCCma-CanESM2	1	0.44° × 0.44°
		CNRM-CERFACS-CNRM-CM5	2	0.44° × 0.44°
		CSIRO-QCCCE-CSIRO-Mk3-6-0	3	0.44° × 0.44°
		NOAA-GFDL-GFDL-ESM2M	4	0.44° × 0.44°
		IPSL-IPSL-CM5A-LR	5	0.44° × 0.44°
		MPI-M-MPI-ESM-MR	6	0.44° × 0.44°

Note: 1: The Canadian Centre for Climate Modelling and Analysis of Environment and Climate Change Canada.
2: Centre National de Recherches Meteorologiques (CNRM) and Centre Europeen de Recherche et Formation Avancees en Calcul Scientifique (CERFACS).
3: Commonwealth Scientific and Industrial Research Organisation (CSIRO, Australia) and Queensland Climate Change Centre of Excellence (QCCCE).
4: The National Oceanic and Atmospheric Administration, Geophysical Fluid Dynamics Laboratory.
5: Institute Pierre Simon Laplace.
6: Max Planck Institute for Meteorology.

greatest absolute difference between observed and expected frequencies across various categories;

$$D = \max_{1 \le i \le N} \left(F(x_i) - \frac{i-1}{N}, \frac{1}{N} - F(x_i) \right) \quad (1)$$

where $F(x_i)$ is the observed and expected frequencies, D indicates the distribution, and N and i are the total number of categories and classes, respectively. The test's null hypothesis states that there is no discernible difference between the theoretical and actual data distributions. Therefore, the Kolmogorov–Smirnov test was recruited in this study to select and fit the most appropriate PDF to the precipitation values of selected stations at probability level $\alpha = 0.05\%$.

2.4. Bias correction method of simulated data

Most GCM/RCM simulations are biased because of problems related to modeling complex climate interactions. The differences between the GCM/RCM simulations and the observational data are caused by the inappropriate resolution of the climate model from the land-surface heterogeneities at the sub-grid scale. Before applying the GCM/RCM datasets in hydrological usages, the bias in them should be corrected. In the research literature, there are several skew correction techniques such as constant scaling, daily scaling, and quantile mapping; nesting bias correction, multivariate recursive nesting bias correction, and conditional quantile-based bias correction are clear (Mehrotra & Sharma 2015). However, in the present study, the quantile ranking-based bias correction (QRBC) technique proposed by Chanda & Maity (2017) was used for correcting the precipitation values.

To determine the QRBC parameters, a suitable PDF is fitted to GCM/RCM simulated and observational datasets for the HP (1976–2005). After that, quantile values of the cumulative distribution function (CDF) obtained from the previous step are divided into ten equal parts between 0 and 1 based on the decimal method. Based on their CDF, the observed and simulated GCM/RCM values are then arranged separately from the lowest to the highest value. Finally, the mean and standard deviation of the observed data and the GCM/RCM simulation in each decile are calculated, and the corrected GCM/RCM value is obtained based on Equation (2):

$$\mathrm{Pr}_{\mathrm{BC}} = \mathrm{Mean}(\mathrm{Pr}^i_{\mathrm{Obs}}) + \left((\mathrm{Pr}^i_{\mathrm{GCM/RCM}} - \mathrm{Mean}(\mathrm{Pr}^i_{\mathrm{GCM/RCM}})) \times \frac{\mathrm{SD}(\mathrm{Pr}^i_{\mathrm{Obs}})}{\mathrm{SD}(\mathrm{Pr}^i_{\mathrm{GCM/RCM}})} \right) \quad (2)$$

where $\mathrm{Pr}^i_{\mathrm{GCM/RCM}}$ represents the raw simulated precipitation values of GCM/RCMs, $\mathrm{Mean}(\mathrm{Pr}^i_{\mathrm{GCM/RCM}})$ represents the average raw values of GCM/RCMs precipitation for the desired quantile interval (here deciles), $\mathrm{Mean}(\mathrm{Pr}^i_{\mathrm{obs}})$ is the mean of the observed precipitation values for the desired quantile intervals, and $\mathrm{SD}(\mathrm{Pr}^i_{\mathrm{obs}})$ and $\mathrm{SD}(\mathrm{Pr}^i_{\mathrm{GCM/RCM}})$ are the standard deviation of the observational and simulated raw data of precipitation for the desired quantile intervals, respectively.

2.5. Modified standardized precipitation index

The standardized precipitation index (SPI) is a tool implemented by McKee *et al.* (1993, 1995) to determine and monitor drought intensities. To determine the SPI at any given timescale, several steps must be taken as follows:

(1) calculating the total cumulative precipitation regarding the desirable timescale;
(2) fitting the gamma distribution functions to the cumulative precipitation;
(3) estimating the distribution function values for whole of the precipitation;
(4) SPI calculation via transferring gamma distribution function values to normal values.

Actually, SPI as a z-score indicates the deviation of an event from the mean, expressed in units of standard deviation (SD). This feature allows comparison between SPI values in different places and periods. Whenever SPI values are continually negative, a drought has occurred. This event finishes when the SPI values become positive. The intensity of droughts is conventionally listed based on this drought index as in Table 3.

Nevertheless, there are various regions in Iran in which the precipitation rate is too low in some months, which leads to an increase in the potential of the number of zero precipitations, chiefly in the short term. This problem is considered one of the significant challenges for allocating SPI values. When there are several zeros in the precipitation distribution, the cumulative

Table 3 | Drought intensity classification based on SPI

SPI classes	SPI values
Extremely wet year	$2 \leq$ SPI
Severely wet year	$1.5 \leq$ SPI ≤ 1.99
Moderately wet year	$1 \leq$ SPI ≤ 1.49
Mildly wet year	$0.5 \leq$ SPI ≤ 0.99
Normal	$-0.49 \leq$ SPI ≤ 0.49
Mild drought	$-0.99 \leq$ SPI ≤ -0.50
Moderate drought	$-1.49 \leq$ SPI ≤ -1
Severe drought	$-1.99 \leq$ SPI ≤ -1.5
Extreme drought	$-2 \leq$ SPI

probability is calculated by Equation (3) as follows:

$$P(x) = p_0 + (1 - p_0)F(x_{p>0}, \lambda) \tag{3}$$

In this scenario, p_0 represents the ratio of zero precipitation values and $F(x_{p>0}, \lambda)$ represents a distribution function calculated from non-zero precipitation data. Because it takes into account the maximum value of SPI value for the zeros group illustrated in the left column of Figure 2, the conventional form of SPI for calculating zeros might be difficult (Stagge *et al.* 2015).

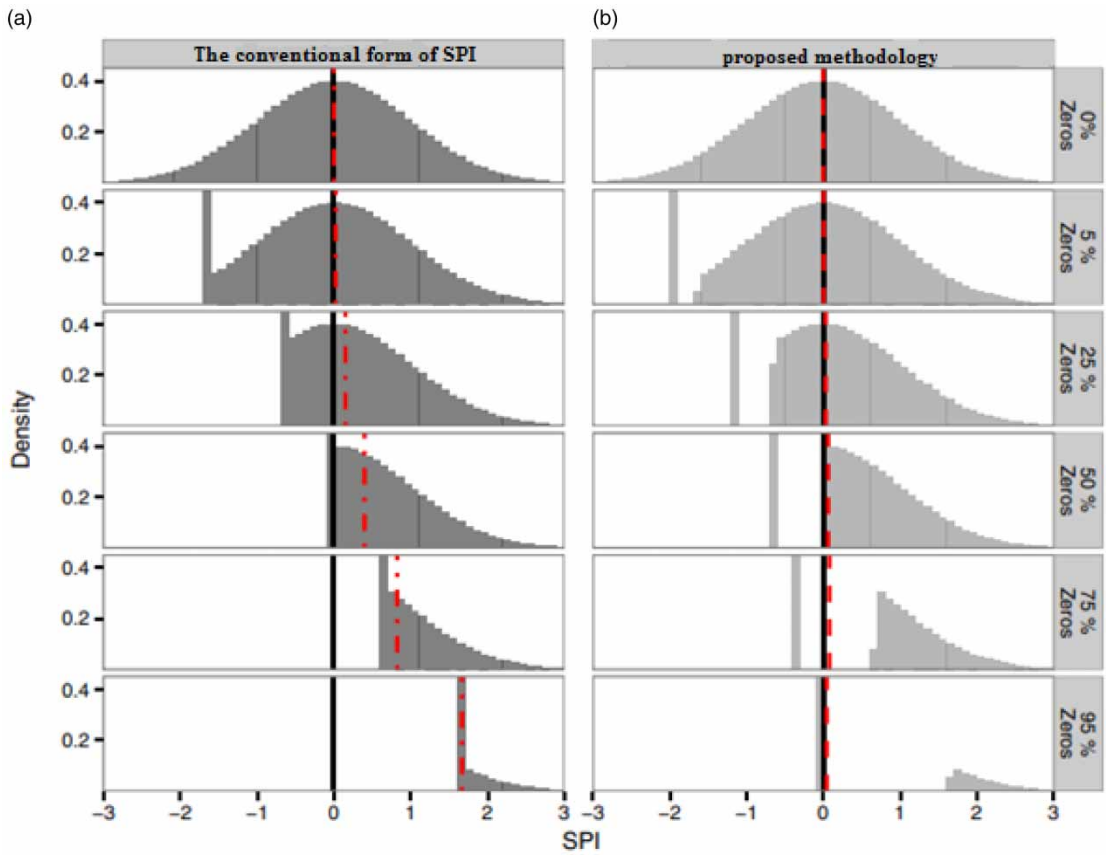

Figure 2 | Simulated SPI distributions with increasing proportions of zero precipitation using (a) the conventional form of SPI and (b) the proposed methodology using Stagge *et al.* (2015). (Black line indicates the mean of SPI with no precipitation of zero. Red dashed line represents the mean of SPI with existence of precipitation of zero.)

In the conventional form of SPI computation, assigning SPI values to zero precipitation values can be a prominent problem since the higher values related to the SPI distribution are increasingly truncated (Figure 2). This goes against one of the main definitions of SPI, which specifies that its mean value is based on 'typical' conditions, 50% of wetter years and another 50% of drier years. Concerning the red dashed line of Figure 2, as the number of zeros rises, so does p_0, increasing the mean SPI computed using the conventional form of SPI method proportionately. Owing to the problems in this technique, another method was proposed using Stagge *et al.* (2015) on the basis of the 'center of mass' of the zero distribution rather than the maximum probability calculation, which has been suggested to allocate SPI values to zero precipitation. By using this strategy, SPI values that correspond to zero precipitation values retain all of their statistical interpretation (mean = 0). In this method, the empirical cumulative distribution is applied to calculate the likelihood of zero precipitation for normalizing zero precipitation.

For instance, for extreme cases, the percentage of zero precipitation is greater than 50% ($p_0 > 50\%$), the computed SPI values will never assign negative values. Therefore, it leads to making an irrational situation, and the entirety of periods that experienced no precipitation will be shown as wetter than usual. Due to lack of information about drought severity and as the precipitation is constant during all periods of zero precipitation, the severity likelihood of drought can be as high as $n_{p=0}/(n+1)$ or as low as $1/(n+1)$. Thus, the average of Weibull nonexceedance probabilities is defined as the center of probability mass for multiple zeros, which is computed as follows (Stagge *et al.* 2015):

$$\bar{p}_0 = \frac{n_{p=0}+1}{2(n+1)} \tag{4}$$

where $\bar{p}_0$ represents the mean probability of multiple zeros according to the function of Weibull plotting position. After that, this computed value is selected for computing the SPI for the center of probability mass for zero precipitation. Consequently, the PD is calculated as follows:

$$p(x) = \begin{cases} p_0 + (1-p_0)F(x_{p>0},\ \lambda), & x > 0 \\ \dfrac{n_{p=0}+1}{2(n+1)} & x = 0 \end{cases} \tag{5}$$

where *F(x,λ)* demonstrates the parametric univariate PD of the samples with detectable cumulative precipitation that matches the parameter λ and p indicates the PD. Accordingly, SPI values for detectable precipitation can be computed using Equation (3). However, the probability of zero precipitation is calculated by Equation (5) according to the mean position of the Weibull plot. It is obvious that the mean SPI value is 0 and the p_0 values can be interpreted (the right side of Figure 2).

Moreover, increasing the p_0 value causes the SPI variance to drop below 1, which is an obvious outcome of any method. In addition, a ratio of zeros can limit the minimum SPI value, which can be the most likely real value. However, the conventional form of SPI computation reaches an infinite SPI that may not be interpretable. For more information, please refer to the study by Stagge *et al.* (2015).

In addition, the conventional form of SPI computation supposes the total of monthly/seasonal precipitation as a unique population. Therefore, the SPI is computed with respect to the SD and the mean of the considered statistical population. This technique does not seem suitable for arid and semi-arid regions, which have not experienced precipitation during various seasons including winter (December to February), spring (March to May), summer (June to August), and autumn (September to November). Hence, owing to the lack of identical distribution of precipitation and the high CV, this kind of precipitation arrangement for these regions causes the wet months/seasons to be more exaggerated in the SPI assigned. However, the importance of the dry months/seasons is reduced in the process of SPI calculation. Accordingly, in this study, each month/season is assumed as an independent population so as to compute SPI for each month/season. Thus, the SPI of each independent population is determined regarding the mean and SD of the selected month/season. Afterward, the calculated SPI values of the independent months/seasons are combined as an integrated statistical population. The precipitation values for the spring season during the specific period are assumed to be a statistical population. Thus, the SPI values for precipitation values during this season are computed. This process is also performed for the remaining seasons (winter, summer, and autumn). Finally, the computed SPI values are combined as an integrated statistical population including winter, spring, summer, and autumn.

Fitting the suitable PDF to precipitation values at various timescales plays a significant role in computing the SPI at each station. Dozens of researchers, such as McKee *et al.* (1993, 1995), have suggested the gamma PD as a proper distribution so as to fit the precipitation values. After that, transference was used from the cumulative probability of the gamma distribution to that of normal distribution (mean = 0 and SD = 1). However, the precipitation values in arid and semi-arid regions might not follow the gamma PD especially at shorter timescales and might have a strong skewness. Hence, for computing the SPI values, various PDFs, namely, logistic, generalized extreme value (GEV), Rayleigh, gamma, exponential, and normal have been selected for fitting to the precipitation time series. Eventually, the combination of three reformations in SPI processing leads to making the modified standardized precipitation index (MSPI).

2.6. Theory of runs

The theory of runs (TOR) relies on the selection of a critical threshold level, y_c. Considering a discrete time series, $x_1, x_2, \ldots, x_i, \ldots, x_n$, a negative (positive) run occurs when x_i is less (or more) than y_c consecutively during one or more time intervals. Negative runs in the SPI time series refer to dry spells, and positive runs refer to wet spells. TOR can be described by characteristics including drought duration, severity, intensity, and frequency (number of drought events) (Guerrero-Salazar & Yevjevich 1975; Wang *et al.* 2020).

A drought frequency (F) is known as a consecutive sequence of a timescale (t) with SPI values less than a considered threshold. Drought duration (D) is a time period between the initiation and termination of a drought that the SPI value is consecutively lower than the critical threshold value. Drought severity (S) is defined as a cumulative deficiency of the SPI values below the critical level (summation of negative SPI values in the drought duration). Drought intensity (I) is computed using the drought severity divided by the drought duration (Zhang *et al.* 2022). These features are graphically presented in Figure 3 for better understanding. In the current study, the three characteristics of drought duration (D), intensity (I), and frequency (F) were extracted for each station at seasonal and annual timescales based on this theory. The critical threshold level, y_c, for extracting these features is SPI 0. In addition, the diagram of variation of projected drought characteristics under the climate change scenarios using MSPI is illustrated in Figure 4.

3. RESULTS AND DISCUSSION

3.1. Investigating the performance of RCMs in simulating station precipitation over the territorial area of Iran

In this section, the simulated precipitation data of RCMs related to CORDEX-SA is compared with the observational data of 39 synoptic stations within the political borders of Iran for the base period of 1976–2005 on a seasonal scale. The results reveal that RCMs do not have a high ability in the simulation of seasonal precipitation in Iran (Figure 5(a)). As shown in

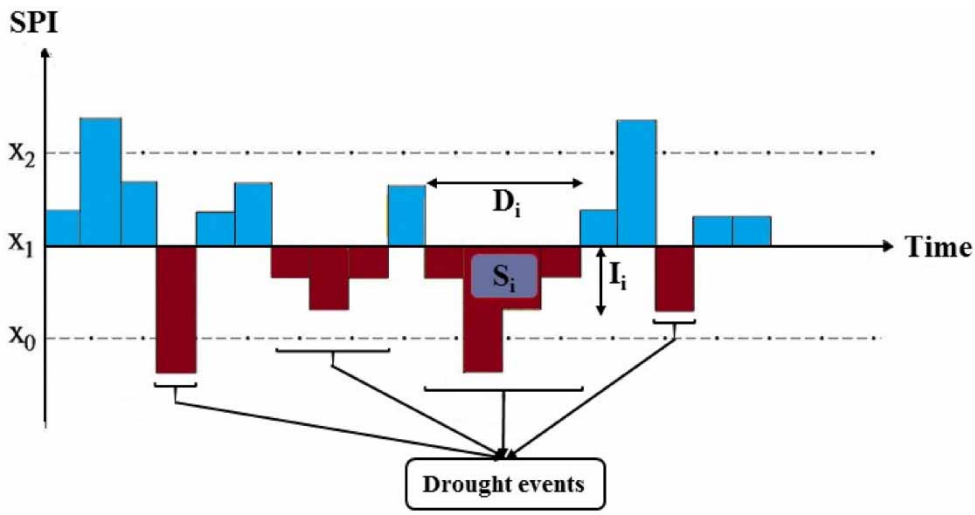

Figure 3 | Hypothetical diagram of determining droughts and their characteristics using the theory of runs. (Duration (D_i) is a time period between the initiation and termination of a drought in which the SPI value is consecutively lower than the critical threshold value; severity (S_i) is summation of negative SPI values in the drought duration; intensity (I) is computed by dividing the drought severity by the drought duration.)

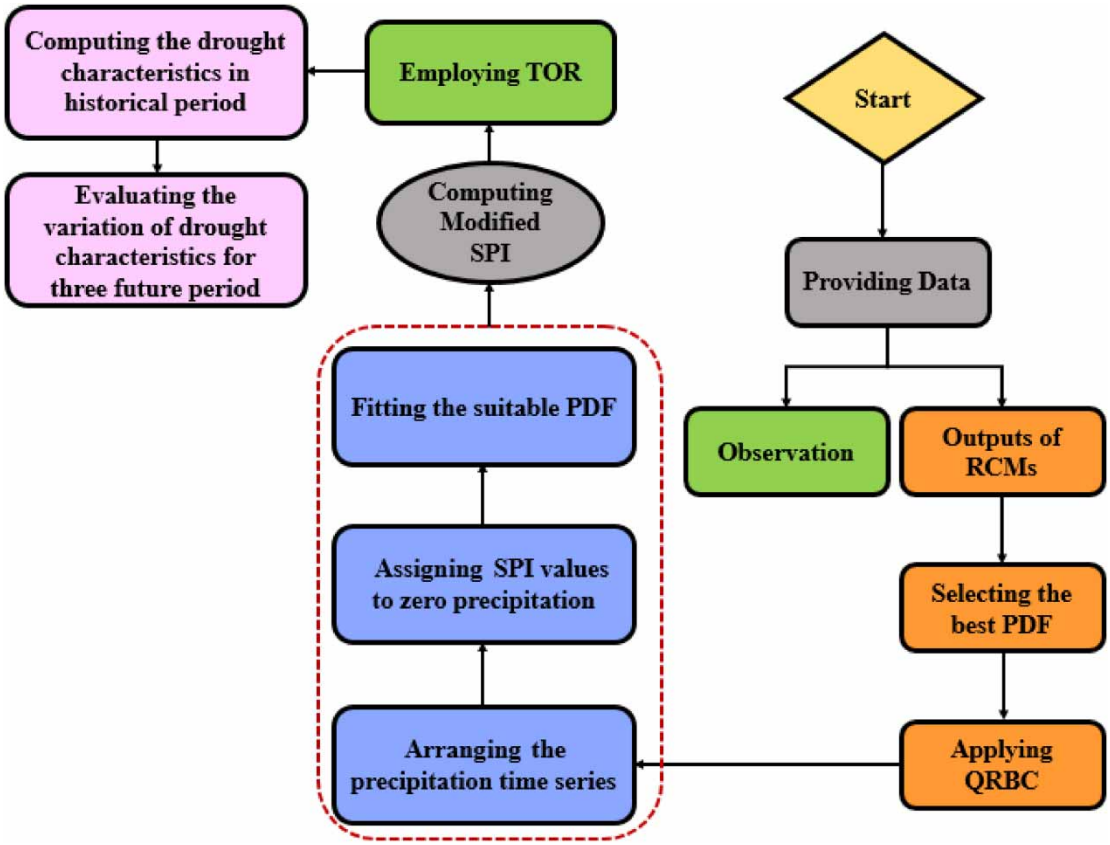

Figure 4 | The diagram of future changes in drought characteristics under the climate change scenarios using MSPI.

Figure 5(a), for most of the stations in Iran, the correlation coefficient between simulated and observational data is between 0.3 and −0.3, which is a very low correlation coefficient. In some regions, such as the west of Iran, high correlation coefficients up to 0.6 are also observed. For bias correction in the simulated data of RCMs used in this study, the QRBC was used. By performing this correction on the simulated data of RCMs, it is observed that the correlation coefficient between the simulated and observational precipitation for all stations is increased to above 0.9 (Figure 5(b)).

Since an index alone cannot be considered a reliable criterion for evaluating the potential of the bias correction method, besides the correlation coefficient (R), the root-mean-square error (RMSE) and the mean absolute error (MAE) are also used (Figure 5(c) and 5(d)). The SD resulting from the evaluation criteria shows that the QRBC method indicated an acceptable performance in simulating seasonal precipitation values and the RMSE and MAE values are between 1 to 28 and 1 to 20 mm, respectively, and the highest calculated RMSE and MAE values are related to the northern regions of Iran (some parts of the Caspian Sea catchment) due to the high seasonal precipitation of these regions compared with the other regions.

3.2. Modified standardized precipitation index (MSPI)

Determining the most appropriate PDF for SPI calculation is one of the prominent challenges in applying SPI for drought monitoring. In this research, various PDFs have been developed to fit to precipitation time-series of each station at both seasonal and annual timescales. In addition, the Kolmogorov–Smirnov test (K-S) has been implemented to investigate the acceptable fit of the best PDFs to the historical data. Thus, six PDFs, namely logistic, GEV, Rayleigh, gamma, exponential, and normal, have been considered at probability level $\alpha = 0.05\%$. In general, the result indicates that the GEV distribution had roughly the best fit to the precipitation values in each season in comparison with other distributions for selected stations. However, due to the remarkable number of zero precipitations for some of the dry stations in summer, the normal distribution was selected to fit precipitation values. Since there is no zero precipitation for annual precipitation, the GEV was the best distribution in fitting the annual precipitation values. The best PDFs selected for SPI computing for the proposed stations at annual and seasonal timescales are provided in Table 4.

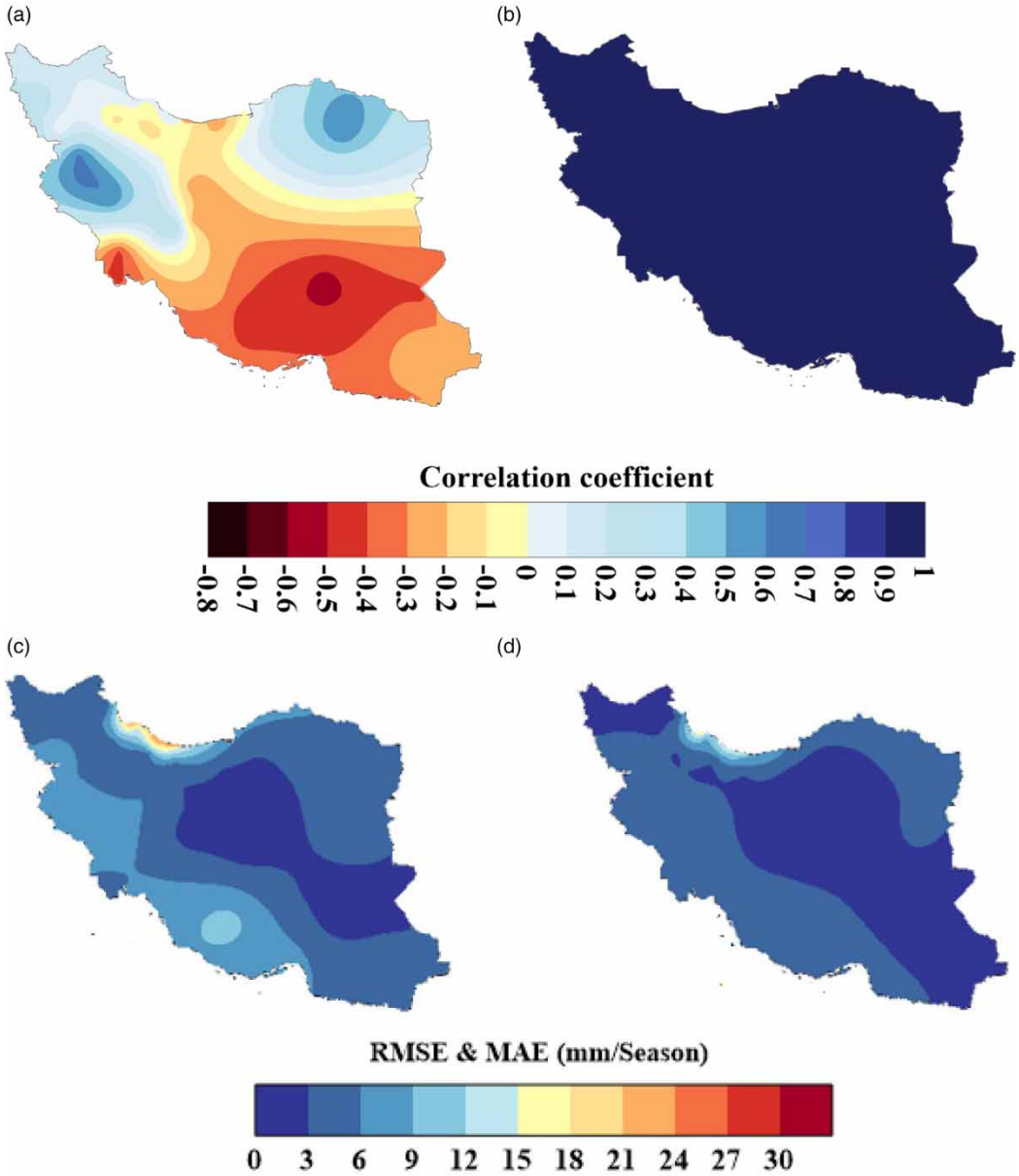

Figure 5 | Spatial distribution of computed correlation coefficient between observed and (a) uncorrected RCMs outputs and corrected RCMs outputs using (b) QRBC, (c) RMSE and (d) MAE values in precipitation simulation at the seasonal timescale.

After determining the best distribution for precipitation values on both seasonal and annual timescales for the observed HP, the seasonal SPI values of Zabol station were computed for each season based on the two selected arrangements (the conventional form of SPI and MSPI) as an example (Figure 6). When it comes to seasonal timescale, there are 120 seasons during a 30-year period of statistical population of precipitation. It should be noted that there are various stations in Iran that have not experienced precipitation during various seasons. For example, Zabol, located in eastern Iran, has never experienced precipitation during 39 seasons of the HP (120 seasons).

As shown in Figure 6, for seasonal scale, various results of SPI were extracted by the two selected arrangements. It is clear on the seasonal SPI that in 'the conventional form of SPI', the SPI computed values are the same for different seasons, whereas in the 'MSPI', these SPI values varied much. This difference among seasonal SPI values is more significant for seasons because summer is known as a dry season in Iran, while a considerable amount of precipitation starts in autumn. The autumn of 1987 was selected as an example of this difference. In the conventional form of SPI, the value of SPI −0.38 is

Table 4 | The best probability distribution functions selected for SPI computing for the proposed stations at annual and seasonal timescales

No	Station	Winter	Spring	Summer	Autumn	Annual
1	Bandar Anzali	4	4	4	4	4
2	Ardebil	4	4	4	4	4
3	Babolsar	4	4	1	3	4
4	Ramsar	6	1	4	4	4
5	Abadan	6	4	6	1	4
6	Ahwaz	4	1	6	4	1
7	Arak	4	4	4	4	4
8	Bam	4	4	4	4	4
9	Bandar Abbas	1	1	4	4	4
10	Bandar Lengeh	4	1	6	4	4
11	Birjand	4	1	6	4	4
12	Bushehr	1	4	6	1	4
13	Esfahan	1	6	4	4	4
14	Fassa	1	5	4	4	4
15	Qazvin	4	4	4	4	4
16	Gorgan	1	4	5	3	4
17	Iranshahr	1	2	4	4	6
18	Kashan	4	4	4	2	4
19	Kerman	4	1	4	4	4
20	Kermanshah	1	1	4	4	4
21	Khoram abad	4	4	4	4	4
22	Khoy	4	6	4	4	4
23	Mashhad	4	4	4	4	4
24	Urmia	4	1	4	4	4
25	Rasht	6	4	4	6	4
26	Sabzevar	3	6	4	1	4
27	Saghez	4	4	3	4	4
28	Sanandaj	4	3	4	4	4
29	Semnan	3	4	4	1	4
30	Shahre Kord	4	1	4	4	4
31	Shahroud	3	4	1	4	4
32	Shiraz	3	3	4	1	4
33	Tabriz	4	4	1	4	4

34	Tehran	3	4	1	1	4
35	Yazd	4	4	6	1	4
36	Zabol	4	2	6	4	4
37	Zahedan	4	1	6	4	4
38	Zanjan	4	1	4	4	4
39	Chabahar	4	4	4	4	4

Distribution	Gamma	exponential	Logistic	Generalized Extreme Value	Rayleigh	Normal
Color	1	2	3	4	5	6

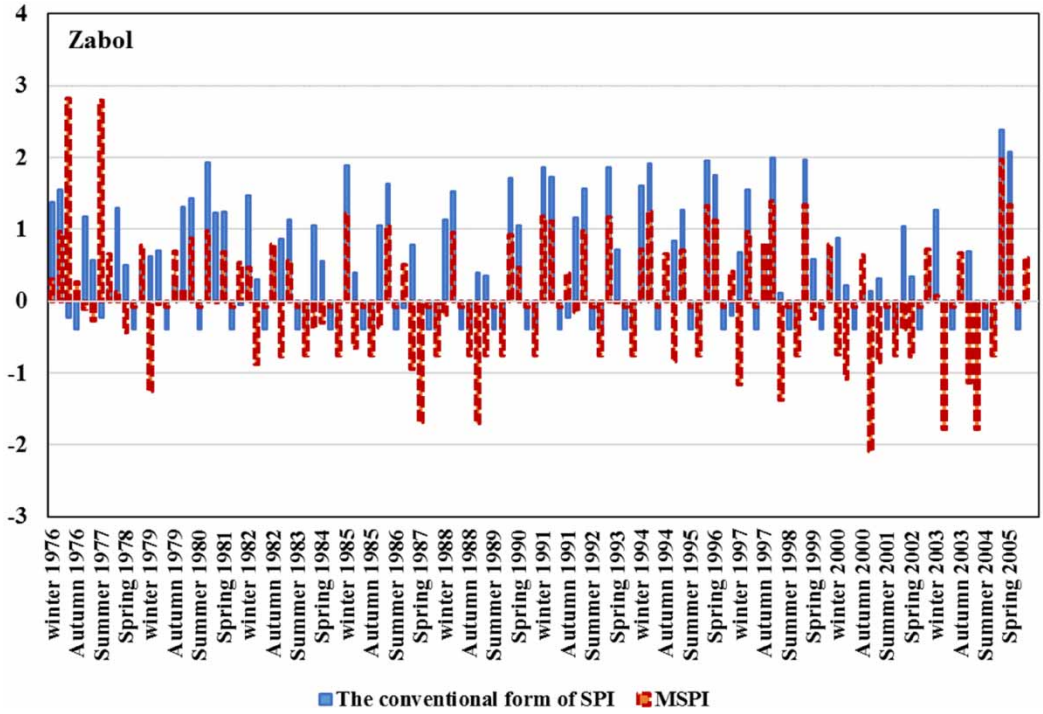

Figure 6 | Comparative graph of seasonal modified SPI time series of Zabol station using 'the conventional form of SPI' and 'MSPI' during HP.

assigned. However, the drought intensity obtained by the MSPI was much more severe than this amount. Moreover, the comparison of the drought characteristics obtained using two selected arrangements during the HP at Zabol station is shown in Table 5. As shown in Table 5, the average drought characteristics achieved by MSPI were significantly more than the conventional form of SPI. For instance, average intensity and duration obtained by MSPI were respectively 20.58% and 38.23% greater than those of the conventional form of SPI for which intensity = −0.34 and duration = 1.7. Regarding the result, MSPI could represent the SPI values better than the conventional form of SPI. Hence, this method was applied to evaluate the changes in drought characteristics for NF, MF, and FF climate periods.

3.3. Changes in drought characteristics of Iran on an annual scale

The average intensity of Iran's annual droughts based on MSPI for all studied stations for the HP (1976–2005), as well as three future climate periods, i.e. NF climate (2010–2039), MF climate (2040–2069), and FF climate (2070–2099), were calculated.

Table 5 | Average of intensity, duration, and frequency of seasonal drought in the historical period at Zabol station

Drought characteristics	The conventional form of SPI	Modified SPI
Intensity	−0.34	−0.41
Duration (season)	1.7	2.35
Frequency	51	73

On a national scale (calculated from the total ratio of the long-term average drought intensity of the studied stations to their number), the average of drought intensity in Iran for the HP was equal to −0.78 (Table 6). Based on this number, the results show that the intensity of droughts in Iran on a national scale under the two scenarios RCP4.5 and RCP8.5 for three future climate periods shows an increase in intensity, and the greatest increase in intensity is related to RCP8.5 for far climate (3.83% increase compared to the HP).

At the station scale, the results show that a significant area of Iran had experienced droughts with a variable range between −0.5 and −1. It is also clear that most of the stations between the Caspian Sea and Central catchments of Iran have received higher drought intensity values in the HP (Figure 7). Currently, based on the intensity of droughts in the HP of the studied stations, the results indicate that based on both RCP4.5 and RCP8.5 scenarios, the southern regions of Iran in the three future climates will face a decrease in the intensity of droughts. Likewise, the stations located in the Gharaghoum catchment (north-eastern regions of Iran) are experiencing a decrease in the intensity of drought in both NF and MF climates, and the range of changes in the intensity of drought can reach 15% compared with the base period. However, based on the results attained in far-future climates, these areas will face increased droughts. In addition, it can be observed that the increase of changes in the intensity of droughts will be experienced in other stations of Iran in the three climates of NF, MF, and FF, whose intensity and extent are different based on RCP8.5 and RCP4.5 scenarios. Put differently, the highest intensity increase in droughts among the studied stations based on the RCP4.5 scenario will occur in Birjand station in the Meshkil and Hamoun catchment (the east of Iran) (32.41% compared with the HP) in the NF climate, while the comparison of drought intensity changes among Iranian stations showed that based on RCP8.5 scenarios, Urmia station in the northwest of Iran (Urmia Lake catchment) will witness the greatest increase in intensity (34.23% compared to the HP) in the MF climate. It must be mentioned that the highest reduction in the intensity of the drought based on the two scenarios RCP4.5 (−21.91% compared with the HP) and RCP8.5 (−36.84% compared with the HP) belongs to Kerman station in the FF climate.

Table 6 | Average of intensity, duration (period considered), and frequency of Iran's droughts on a national scale during HP and their changes in NF, MF, and FF climates for annual and seasonal timescales

Period	Scenario	Intensity (%)	Duration (%)	Frequency (%)
Annual timescale				
Historical	–	−0.78	2.35	15.10
Near future	RCP 4.5	2.08	−0.96	−0.44
	RCP 8.5	2.05	−1.65	−0.66
Mid-future	RCP 4.5	0.67	−2.04	−0.07
	RCP 8.5	3.53	−1.71	−1.5
Far future	RCP 4.5	1.99	1.24	0.58
	RCP 8.5	3.83	0.38	−0.91
Seasonal timescale				
Historical	–	−0.76	2.03	57.90
Near future	RCP 4.5	8.55	−0.15	1.41
	RCP 8.5	8.99	0.23	1.78
Mid-future	RCP 4.5	11.32	0.22	0.95
	RCP 8.5	9.29	0.94	2.04
Far future	RCP 4.5	9.71	0.71	2.08
	RCP 8.5	10.97	−0.01	1.55

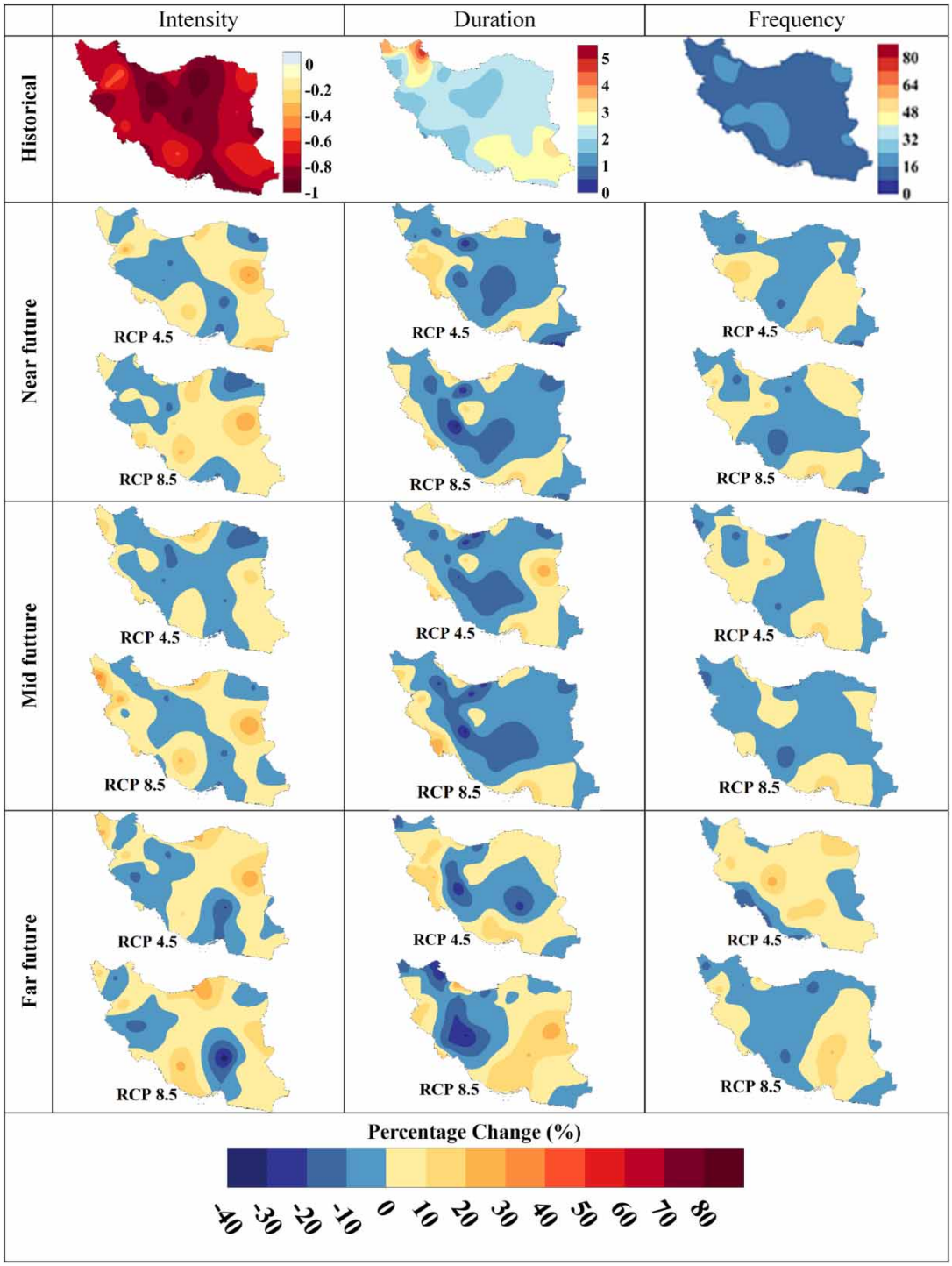

Figure 7 | Spatial distribution of intensity, duration, and frequency of Iran's annual droughts during the historical period and their changes in the near-future, mid-future, and far-future climates.

Table 6 also presents the average length of drought periods in the HP and their average changes until the year 2100. It can be said that the average duration of drought in Iran is 2.35 years. Figure 7 depicts the SD of Iran's drought period during the HP. Based on Figure 7, the duration of drought periods in Iran has varied between 1.5 and five years, and the longest drought periods have occurred in the northwestern regions of Iran, which have been associated with the highest intensity of drought.

The stations located in the western regions (some regions of the Persian Gulf catchment) have experienced a shorter period of drought compared with the average length of the drought period in Iran (2.35) and the intensity of the drought in these regions has been lower compared with the other stations in Iran. Using the output results, it was determined that the changes in the average length of the dry spell for Iran in the NF climate in the RCP4.5 scenario will be −0.96%, and despite the decrease in the average length of the drought period in Iran, the western regions of Iran (located in the Persian Gulf catchment) such as Abadan and Sanandaj will experience the increased length of the drought period. In the meantime, in the next period (MF climate), the eastern regions (Meshkil and Hamoun catchment) will witness an increase in the drought duration, and the length of the drought period in the western regions will decrease compared with the NF climate. Unlike the two NF and MF climates, Iran, being in the FF climate, will witness a 1.24% increase in the changes in the length of the drought period compared with the base period, and except for the areas that are near the Alborz and Zagros mountain ranges, the range of changes in the length of the drought period will reach up to 15% in most regions. By comparing the two scenarios RCP4.5 and RCP8.5, it was also clarified that the changes in the length of the drought period under the RCP8.5 scenario will be less than under RCP4.5. In the RCP8.5 scenario, the western and southern regions (Persian Gulf catchment) will face increased changes in the duration of the dry spell in 2040–2070, and being in the FF climate, the duration of the drought period in the western regions will decrease, but the significant increase in the drought duration will affect the eastern regions.

In line with the frequency of droughts, it can be mentioned that the average frequency of droughts in Iran was 15.10 cases in the HP, and the variety of drought frequency for most stations in Iran was between 12 and 16 cases. Based on the RCP4.5 scenario, until 2040, the northern to southwestern regions of Iran will see a decrease in the frequency of droughts. In the MF climate, the frequency of droughts will increase in the northeastern and northwestern stations, and when reaching the FF climate, the frequency of droughts will decrease in the northeastern and southwestern regions. While the south, southeast, and west regions (Persian Gulf and Meshkil and Hamoun catchments) with an arid climate will be associated with an increase in the frequency of droughts in NF, MF, and FF climates, the increase of changes in the western regions will reach approximately 20%. The results from Table 6 and Figure 7 show that the RCP8.5 scenario shows the frequency of droughts in western stations to be less than in the RCP4.5 scenario, and the frequency of droughts in all future climates has decreased under the pessimistic scenario of RCP8.5. This decreasing trend reaches its maximum (1.5%) in the MF climate, and the number of stations that have a decreasing trend will increase.

3.4. Changes in intensity, duration, and frequency of droughts in Iran on a seasonal scale

The average intensity of seasonal droughts in Iran was calculated based on SPI for all studied stations for the HP and three future climate periods. The average intensity of droughts in Iran on a national scale for the HP was equal to −0.76. The intensity of Iran's droughts on a national scale will increase under RCP4.5 and RCP8.5 scenarios for the three climates of NF, MF, and FF. Based on the RCP4.5 scenario, the greatest increase in intensity (11.32% increase compared with the HP) is predicted for the MF climate, while the lowest intensity increase (8.55% increase compared with the HP) is predicted for the NF climate (Table 6). At the catchment scale, the results show that some parts of the Gharaghoum and Central catchments of Iran have witnessed higher drought intensity in the HP (Figure 8). Currently, regarding the intensity of droughts in the HP of the studied stations, the results show that based on the two scenarios RCP4.5 and RCP8.5, the northeast regions and parts of the west, northwest, and the southern coastal strip of the Caspian Sea will face a decrease in the intensity of droughts in the considered future climates. However, the eastern and southwestern stations of Iran will face an increase in the intensity of droughts in the three climates of the NF, MF, and FF, and the range of changes in the intensity of drought in these areas will be up to 91% in the MF climate. Put differently, the highest increase and decrease in intensity (approximately 91% and −24% compared with the HP) will be experienced in Zabol (in the Meshkil and Hamoun catchment) and Sabzevar (in the Gharaghoum catchment) stations, respectively, in the MF climate.

Table 6 presents the average length of the drought period in the HP on a seasonal scale and their average changes until the year 2100. It can be said that the average length of Iran's drought is 2.03 seasons. Figure 8 shows the SD of Iran's drought period during the HP. Based on Figure 8, the length of drought periods in Iran has varied between 1.5 and 2.5 seasons, and the longest drought periods have occurred in the Persian Gulf catchment and Urmia Lake catchment. The range of changes in the average length of the dry spell of Iran on a national scale in the three future climates in the two scenarios RCP4.5 and RCP8.5 is between −0.15% and 0.94%, which indicates insignificant changes in the length of the drought period compared with the HP and the highest and lowest increase of changes will happen in the NF and MF climates, respectively. As shown in Figure 8, it can be stated that despite the increase in drought intensity changes in the southwestern to northwestern regions and parts of eastern

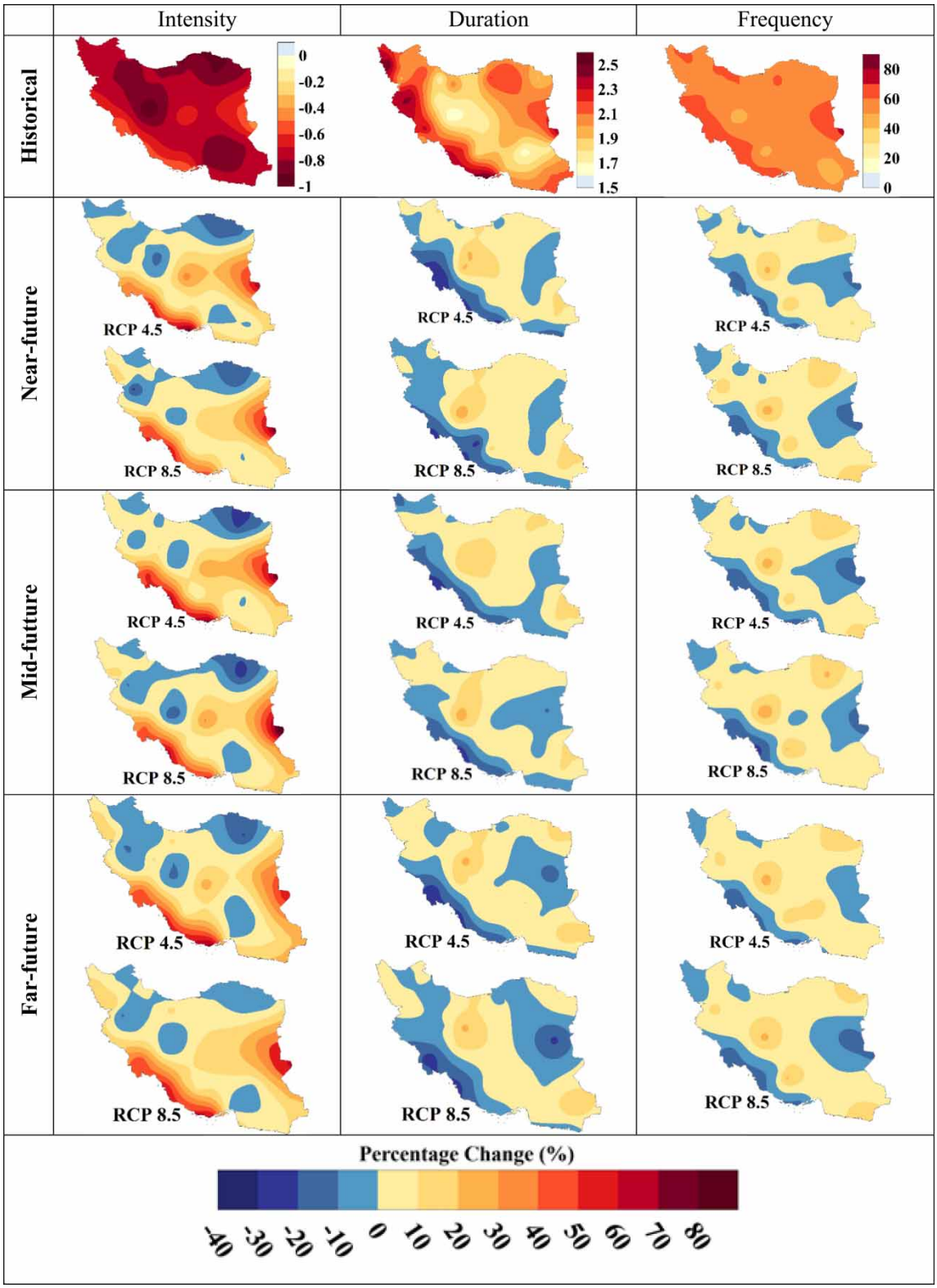

Figure 8 | Spatial distribution of intensity, duration, and frequency of Iran's seasonal droughts during the historical period and their changes in the near-future, mid-future, and far-future climates.

Iran, the duration of the drought period will decrease and the greatest decrease in the changes in the duration of the dry spell will occur in the southwest of Iran (areas that will face the highest increase in intensity). Likewise, with time, the number of stations in the eastern regions of Iran (Meshkil and Hamoun catchment), which face the reduction of changes in the length of the dry spell, will be increased, while the length of the dry period in the northeastern regions (Gharaghoum catchment) to the center of Iran (Central catchment) will increase compared with the HP.

The results of the droughts frequency on a seasonal scale show that the average frequency of drought in Iran was 57.90 cases in the HP, the frequency of droughts in Iran's stations varied between 46 and 73 cases, and the highest frequency of droughts was in some parts of the Persian Gulf (the south to the west of Iran) and Meshkil and Hamoun (eastern regions of Iran) catchments like Zabol. Based on this number, it is very evident that the frequency of droughts in Iran will increase on a national scale under RCP4.5 and RCP8.5 scenarios for the three NF, MF, and FF climates, and the minimum and maximum changes in the frequency of droughts are equal to 0.95% and 2.08% increase compared with the HP, which is related to the RCP4.5 scenario for the MF and FF climates, respectively (Table 6). Based on RCP4.5 and RCP8.5 scenarios, in the three future climates, the eastern regions and parts of the southern to western regions of Iran will see a decrease in the frequency of droughts, so in some southwestern regions of Iran, such as Bushehr, the frequency of droughts will decrease by 25% compared with the HP, while the frequency of droughts will increase in other stations of Iran, especially stations in the Gharaghoum and Central catchments (northeast and central regions of Iran). According to the RCP8.5 scenario, the highest increase in changes (29% increase compared with the HP) will occur in Isfahan in the MF climate (Figure 8).

3.5. Discussion

Due to some limitations of SPI (e.g. the number of zero values in precipitation time-series, considering the appropriate PDF, and suitable arrangement of precipitation time-series), computed SPI values may be incorrect. Therefore, SPI calculation was modified based on the existence of zero precipitation in time-series, the most appropriate PDF, and a proper arrangement for precipitation time-series. Then, spatiotemporal variation of projected drought characteristics under the climate change scenarios was conducted using MSPI.

Moreover, few studies can be found that have predicted changes in characteristics of future droughts for the whole of Iran, and it can be said that the results of this study are consistent with the results of previous studies. For instance, this study can be consistent with the study by Senatore *et al.* (2019), who predicted severe droughts over Iran in the FF using the Palmer drought intensity index (PDSI). Likewise, the SPI outcomes of the study by Fattahi *et al.* (2015), who used the output of the HadCM3 model, indicated that the annual drought intensity will increase during 2011–2030 in western regions of Iran. Two drought indexes including SPI and SPEI in the study by Mesbahzadeh *et al.* (2020) indicated that Yazd province will face increased changes in drought intensity and duration in future compared with the HP. The outcomes of the PDSI projection presented by Dehghan *et al.* (2020) demonstrated that the southwestern regions of Iran (such as Abadeh and Lar) will face dry periods during the next three decades compared with the HP under RCP4.5 and RCP8.5 scenarios.

The study by Zarrin & Dadashi-Roudbari (2021b), which was conducted with CMIP5 models, showed that the intensity and frequency of droughts in Iran will increase in the future climate, which can be considered a significant threat to water resources. Thus, considerable attention to drought management in this country is required. The results of the study by Mirakbari & Ebrahimi-Khusfi (2021) showed that based on the results of SPEI and reconnaissance drought index (RDI), long-term droughts in the eastern wetlands will have a higher intensity and duration than in the HP compared with the western wetlands of Iran. It was also found that severe droughts will be experienced in the southeastern wetlands of Iran in the future. The study by Ghazi *et al.* (2023) performed with CMIP6 models revealed that based on a six-month timescale SPI, SSP5–8.5 scenarios projected more 'extremely dry' events in northwestern stations.

In addition, few studies can be found for which the results are not consistent with the results of this study. For instance, Ahmadebrahimpour *et al.* (2019) projected that, based on the outcomes of SPI and SPEI, drought frequency will increase in the RCP8.5 scenario in northwestern stations until 2100. By using SPI outcomes, Koohi & Etedali (2023) found that the northern regions of Karoun River Basin will face increased change in drought frequency at the end of the 21st century under RCP4.5 and RCP8.5 scenarios.

4. CONCLUSION

- This study can be considered a comprehensive study of the effect of climate change on the various characteristics of droughts in Iran until the end of the 21st century, based on the simulations conducted in the framework of the

CORDEX-SA experiment. The initial evaluation of the performance of RCMs in the HP showed that RCMs performed poorly in simulating Iran's precipitation.

- Average changes in drought characteristics on a national scale revealed that Iran will witness an increase in the intensity and a decrease in the duration and frequency of droughts compared with the HP in the NF and MF climates.
- Scrutinizing the changes in Iran's annual droughts at the station scale also in future climates shows that the southern regions of Iran according to the two scenarios RCP4.5 and RCP8.5 have droughts with less intensity but more duration and frequency of occurrence than in the HP.
- Some parts of Urmia Lake catchment (northwestern regions of Iran) will face increased changes in the intensity and reduced changes in the duration and frequency of droughts by the year 2100.
- Some parts of the eastern and southwestern regions of Iran (Persian Gulf and Meshkil and Hamoun catchments) will face increasing intensity and decreasing duration and frequency of drought compared with the HP, but the intensity, duration, and frequency of droughts in the FF climate will increase compared with the HP.
- Average changes in intensity, duration, and frequency of Iran's seasonal droughts on a national scale indicated that Iran will experience an increase in the intensity, duration, and frequency of drought in all future climates.
- At the station scale, more different results have been obtained among the studied stations in Iran, and the stations in the Persian Gulf and Meshkil and Hamoun catchments face the biggest changes in the intensity of drought compared with the HP. The changes in the duration and frequency of droughts in these regions will be reduced in the three considered climates.
- Even though less severe droughts will affect the Gharaghoum catchment (northeastern regions of Iran), compared with the HP, their duration and frequency will increase.
- The Central catchment of Iran will face increased changes in the intensity, duration, and frequency of droughts by the year 2100.

Based on these changes, it can be concluded that most of Iran will face many problems in the coming years because of the changes in the characteristics of droughts, and strategies should be adopted to better manage water resources and reduce the consequences of droughts. It must be mentioned that drought can affect the Persian Gulf and Meshkil and Hamoun catchments of Iran, which experience the least amount of precipitation in summer, more than other areas. Special attention should be paid to these areas to reduce the consequences of drought.

ACKNOWLEDGEMENTS

The authors thank the World Climate Research Programme's Working Group on Regional Climate, the Working Group on Coupled Modelling that formerly coordinated CORDEX. The authors also thank the Climate Data Portal at the Center for Climate Change Research (CCCR), Indian Institute of Tropical Meteorology, for provision of CORDEX-SA data.

FUNDING

No funding was received to assist with the preparation of this manuscript.

ETHICAL APPROVAL AND CONSENT TO PARTICIPATE

This manuscript does not report on or involve the use of any animal or human data or tissue.

AUTHORS CONTRIBUTIONS

Conceptualization: Alireza Ghaemi, Seyed Arman Hashemi Monfared, Abdolhamid Bahrpeyma, Mohammad Zounemat-Kermani, and Peyman Mahmoudi; methodology: Alireza Ghaemi and Peyman Mahmoudi; data curation: Alireza Ghaemi, Peyman Mahmoudi, and Seyed Arman Hashemi Monfared; writing – original draft preparation: Alireza Ghaemi; writing – review and editing: Seyed Arman Hashemi Monfared, Abdolhamid Bahrpeyma, Mohammad Zounemat-Kermani, and Peyman Mahmoudi; project administration: Seyed Arman Hashemi Monfared. All authors have read and agreed to the published version of the manuscript.

CODE AVAILABILITY

Calculations have been made with Custom codes.

DATA AVAILABILITY STATEMENT

Data cannot be made publicly available; readers should contact the corresponding author for details.

CONFLICT OF INTEREST

The authors declare there is no conflict.

REFERENCES

Ahmadebrahimpour, E., Aminnejad, B. & Khalili, K. 2019 Assessing future drought conditions under a changing climate: a case study of the Lake Urmia basin in Iran. *Water Supply* **19** (6), 1851–1861.

Araghi, A., Martinez, C. J., Adamowski, J. & Olesen, J. E. 2018 Spatiotemporal variations of aridity in Iran using high-resolution gridded data. *International Journal of Climatology* **38** (6), 2701–2717.

Bari Abarghouei, H., Asadi Zarch, M. A., Dastorani, M. T., Kousari, M. R. & Safari Zarch, M. 2011 The survey of climatic drought trend in Iran. *Stochastic Environmental Research and Risk Assessment* **25**, 851–863.

Chanda, K. & Maity, R. 2017 Assessment of trend in global drought propensity in the twenty-first century using drought management index. *Water Resources Management* **31**, 1209–1225.

Dai, A. 2011 Drought under global warming: a review. *Wiley Interdisciplinary Reviews: Climate Change* **2** (1), 45–65.

Dai, A. 2012 Increasing drought under global warming in observations and models. *Nature Climate Change* **3**, 52–58.

Dehghan, S., Salehnia, N., Sayari, N. & Bakhtiari, B. 2020 Prediction of meteorological drought in arid and semi-arid regions using PDSI and SDSM: a case study in Fars Province, Iran. *Journal of Arid Land* **12**, 318–330.

Fang, J., Kong, F., Fang, J. & Zhao, L. 2018 Observed changes in hydrological extremes and flood disaster in Yangtze River Basin: spatial–temporal variability and climate change impacts. *Natural Hazards* **93**, 89–107.

Fattahi, E., Habibi, M. & Kouhi, M. 2015 Climate change impact on drought intensity and duration in west of Iran. *Journal of Earth Science and Climatic Change* **6**, 319.

Ghazi, B., Dutt, S. & Torabi Haghighi, A. 2023 Projection of future meteorological droughts in Lake Urmia Basin, Iran. *Water* **15** (8), 1558.

Gu, H., Yu, Z., Wang, G., Wang, J., Ju, Q., Yang, C. & Fan, C. 2015 Impact of climate change on hydrological extremes in the Yangtze River Basin, China. *Stochastic Environmental Research and Risk Assessment* **29**, 693–707.

Guerrero-Salazar, P. L. A. & Yevjevich, V. M. 1975 *Analysis of Drought Characteristics by the Theory of Runs*. Hydrology Papers 80, Colorado State University, Fort Collins, CO, USA.

IPCC 2012 *Managing the Risks of Extreme Events and Disasters to Advance Climate Change Adaptation. Special Report of the Intergovernmental Panel on Climate Change* (Field, C. B., Barros, V., Stocker, T. F., Qin, D., Dokken, D. J., Ebi, K. L., Mastrandrea, M. D., Mach, K. J., Plattner, G.-K., Allen, S. K., Tignor, M. & Midgley, P. M., eds), Cambridge University Press, Cambridge, UK and New York, NY, USA.

Karamouz, M., Nazif, S. & Falahi, M. 2013 *Hydrology and Hydroclimatology: Principles and Applications*. CRC Press, Boca Raton, FL, USA.

Khazanedari, L., Abasi, F., Ghandhari, S., Kouhi, M. & Malbousi, S. 2009 Drought conditions in the next thirty years in Iran. *Journal of Geography and Regional Development* **7** (12), 83–98 (in Persian).

Koohi, S. & Etedali, H. R. 2023 Future meteorological drought conditions in southwestern Iran based on the NEX-GDDP climate dataset. *Journal of Arid Land* **15** (4), 377–392.

Kottek, M., Grieser, J., Beck, C., Rudolf, B. & Rubel, F. 2006 World map of the Köppen-Geiger climate classification updated. *Meteorologische Zeitschrift* **15** (3), 259–263.

Mahmoudi, P. & Rigi Chahi, A. 2019 Climate change impact on spatial and temporal distribution of precipitation in Iran. In: *6th International Regional Conference on Climate Change*, November 18–19, Tehran, Iran.

McKee, T. B., Doesken, N. J. & Kleist, J. 1993 The relationship of drought frequency and duration to time scale. In: *Proceedings of Eighth Conference on Applied Climatology*, American Meteorological Society Boston, MA, USA, pp. 179–184.

McKee, T. B., Doesken, N. J. & Kleist, J. 1995 Drought monitoring with multiple time scales. In: *Proceedings of Ninth Conference on Applied Climatology*, American Meteorological Society, Boston, MA, USA, pp. 233–236.

Mehrotra, R. & Sharma, A. 2015 Correcting for systematic biases in multiple raw GCM variables across a range of timescales. *Journal of Hydrology* **520**, 214–223.

Mesbahzadeh, T., Mirakbari, M., Mohseni Saravi, M., Soleimani Sardoo, F. & Miglietta, M. M. 2020 Meteorological drought analysis using copula theory and drought indicators under climate change scenarios (RCP). *Meteorological Applications* **27** (1), e1856.

Mirakbari, M. & Ebrahimi-Khusfi, Z. 2021 Evaluation of the climate change effects on the future drought characteristics of Iranian wetlands. *Arabian Journal of Geosciences* **14**, 2167.

Nouri, M. & Homaee, M. 2020 Drought trend, frequency and extremity across a wide range of climates over Iran. *Meteorological Applications* **27** (2), e1899.

Romanowicz, R. J., Bogdanowicz, E., Debele, S. E., Doroszkiewicz, J., Hisdal, H., Lawrence, D., Meresa, H. K., Napiórkowski, J. J., Osuch, M., Strupczewski, W. G., Wilson, D. & Wong, W. K. 2016 Climate change impact on hydrological extremes: preliminary results from the Polish–Norwegian Project. *Acta Geophysica* **64**, 477–509.

Senatore, A., Hejabi, S., Mendicino, G., Bazrafshan, J. & Irannejad, P. 2019 Climate conditions and drought assessment with the Palmer Drought Severity Index in Iran: evaluation of CORDEX South Asia climate projections (2070–2099). *Climate Dynamics* **52**, 865–891.

Shahid, S., Wang, X. J., Harun, S. B., Shamsudin, S. B., Ismail, T. & Minhans, A. 2016 Climate variability and changes in the major cities of Bangladesh: observations, possible impacts and adaptation. *Regional Environmental Change* **16**, 459–471. https://doi.org/10.1007/s10113-015-0757-6.

Stagge, J. H., Tallaksen, L. M., Gudmundsson, L., Van Loon, A. F. & Stahl, K. 2015 Candidate distributions for climatological drought indices (SPI and SPEI). *International Journal of Climatology* **35** (13), 4027–4040.

Su, B., Huang, J., Mondal, S. K., Zhai, J., Wang, Y., Wen, S., Gao, M., Lv, Y., Jiang, S., Jiang, T. & Li, A. 2021 Insight from CMIP6 SSP-RCP scenarios for future drought characteristics in China. *Atmospheric Research* **250**, 105375.

Swain, D. L., Horton, D. E., Singh, D. & Diffenbaugh, N. S. 2016 Trends in atmospheric patterns conducive to seasonal precipitation and temperature extremes in California. *Science Advances* **2** (4), e1501344.

Tabari, H. & Willems, P. 2018 More prolonged droughts by the end of the century in the Middle East. *Environmental Research Letters* **13**, 104005. doi 10.1088/1748-9326/aae09c.

Trenberth, K. E., Dai, A., van der Schrier, G., Jones, P. D., Barichivich, J., Briffa, K. R. & Sheffield, J. 2014 Global warming and changes in drought. *Nature Climate Change* **4**, 17–22. https://doi.org/10.1038/nclimate2067.

Wang, L., Yuan, X., Xie, Z., Wu, P. & Li, Y. 2016 Increasing flash droughts over China during the recent global warming hiatus. *Scientific Reports* **6**, 30571. https://doi.org/10.1038/srep30571.

Wang, L., Zhang, X., Wang, S., Salahou, M. K. & Fang, Y. 2020 Analysis and application of drought characteristics based on theory of runs and copulas in Yunnan, Southwest China. *International Journal of Environmental Research and Public Health* **17** (13), 4654.

Waseem, M., Ajmal, M., Ahmad, I., Khan, N. M., Azam, M. & Sarwar, M. K. 2021 Projected drought pattern under climate change scenario using multivariate analysis. *Arabian Journal of Geosciences* **14**, 544. https://doi.org/10.1007/s12517-021-06860-7.

Yao, N., Li, L., Feng, P., Feng, H., Li Liu, D., Liu, Y., Jiang, K., Hu, X. & Li, Y. 2020 Projections of drought characteristics in China based on a standardized precipitation and evapotranspiration index and multiple GCMs. *Science of the Total Environment* **704**, 135245.

Zarrin, A. & Dadashi-Roudbari, A. 2021a Projected consecutive dry and wet days in Iran based on CMIP6 bias-corrected multi-model ensemble. *Journal of the Earth and Space Physics* **47** (3), 561–578 (in Persian).

Zarrin, A. & Dadashi-Roudbari, A. 2021b Drought risk management in a changing climate: the role of national policies and the Drought Management Plan (DMP). *Journal of Water and Sustainable Development* **8** (1), 107–112.

Zarrin, A. & Dadashi-Roudbari, A. 2021c Projection of drought indices in Iran based on CMIP5 multi-model ensemble. *Climate Change Research* **2** (7), 71–82.

Zhai, J., Mondal, S. K., Fischer, T., Wang, Y., Su, B., Huang, J., Tao, H., Wang, G., Ullah, W. & Uddin, M. J. 2020 Future drought characteristics through a multi-model ensemble from CMIP6 over South Asia. *Atmospheric Research* **246**, 105111.

Zhang, R., Qu, Y., Zhang, X., Wu, X., Zhou, X., Ren, B., Zeng, J. & Wang, Q. 2022 Spatiotemporal variability in annual drought severity, duration, and frequency from 1901 to 2020. *Climate Research* **87**, 81–97.

First received 9 August 2023; accepted in revised form 4 February 2024. Available online 17 February 2024